Application of Dye- Sensitized Solar Cell Technology in the Tropics: Effects of Radiation Intensity and Temperature on DSSC Performance

Article · January 2012

CITATIONS
0

READS
147

1 author:

Raphael Makokha
African PRIDE Centre, Kenya, Emuhaya
4 PUBLICATIONS **6** CITATIONS

SEE PROFILE

Application of Dye-Sensitized Solar Cell Technology in the Tropics: Effects of Radiation Intensity and Temperature on DSSC Performance

Otakwa R. V. M*; Simiyu, J.; Waita, S. M. and Mwabora J. M

Department of Physics, College of Physical and Biological Sciences, University of Nairobi,
PO Box 30197 – 00100 GPO, Nairobi, KENYA
*Corresponding author: raphael.makokha@yahoo.com

Abstract - effects of radiation intensity and temperature on the performance of a dye-sensitized solar module (DSSM) have been investigated in a tropical area in Nairobi, Kenya. Outdoor measurements were performed on cloudless days at normal incidence of the incoming solar beam radiation to the module. A series of current-voltage (*I-V*) characterizations were carried out at different solar radiation intensities and module temperatures. The module performance parameters: Short circuit current density, (J_{sc}), Open circuit voltage, (V_{oc}), Fill factor, (*FF*) and solar-to-electricity conversion efficiency, (η) were extracted from the *I-V* curves. Better efficiencies were observed at lower than higher radiation intensities. There was also an overall improved performance at elevated temperatures. The results may be useful during fabrication of dye-sensitized solar cells meant for use in the tropics.

***Index Terms*— Dye-sensitized, performance, radiation, temperature, tropics**

I. INTRODUCTION

The need to switch to the use of renewable energy is ever increasing. Fossil fuel reserves that have been depended upon to provide the world's energy are quickly diminishing [1][2]. This decline has amplified costs of fossil fuel exploration and mining [1]. The sensitive geopolitical issues experienced by countries with fossil fuel reserves [3] make the situation worse. These matters have contributed to the escalation of energy costs that have pushed energy out of reach for many people. Those at the bottom of the economic pyramid are the worst affected [4].

The over-reliance upon fossil fuels by the world [5] has also been linked to the increase in acid rains, greenhouse gases and depletion of the ozone layer [6]. Impacts of greenhouse gases, e.g., global warming have been widespread [7] [8].They have adversely affected life on earth [9]. Adoption of energy sources that are alternative to fossil fuels and renewable in nature is imperative. These renewable energy sources include biomass, geothermal, tidal, water cycle or hydro, atmospheric movements and solar radiation [10]. They are consequences of the earth's inherent heat, gravitational perturbations by the moon and sun, and solar radiation [11].

The most abundant and fairly distributed of these is solar radiation with about 3.9×10^{24} joules of solar energy reaching the earth annually [12]. This impressive supply of solar energy is complemented by its vast resourcefulness – it can be converted into electricity by exciting electrons in a solar cell and can also yield chemical fuel through natural photosynthesis in green plants or artificial photosynthesis in human-engineered systems. Solar energy can also be used to produce heat for direct use or for further conversion to electricity [12].

Though the prices of solar photovoltaic (PV) systems are currently high [14], investing in solar power assures free energy after a reasonable payback period. This makes solar electricity both cost effective and economical [15] in the long run. Solar energy is also environmentally friendly [16] and can be availed even to the remotest parts of the world. [17] has attributed this to the minimal incidences of wear and tear by solar energy systems since they do not comprise of heavy moving parts. Solar energy is also free, abundant, readily available, and does not interfere with people's ways of life. Generation of electricity from solar energy is therefore a socially, politically, economically, environmentally and culturally (SPEEC) attractive method of directly generating electrical power.

Reduction in solar energy cost will enhance its penetration, especially among the poor. This in turn will improve the ecological footprint of communities, nations and the world. Though first generation silicon solar devices dominate the PV market currently, their fabrication costs are high, which calls for high efficiencies [18]. This translates to high prices, hence choking their penetration to the poor. Second generation

solar devices are also expensive to fabricate. Third generation solar cells, the dye-sensitized solar cell are cheaper alternatives to the conventional silicon solar cells as well as the second generation solar cells, and can be fabricated under less stringent conditions [19]. They are therefore favorable in taking up the huge energy opportunities that exist in the tropics. They have however not been field-tested in the tropics, which is the focus of this study.

II. MATERIALS AND METHODS

A. Basic Theory

1) J-V characterization

The response of a PV device is determined by its *J-V* characteristics both in the dark and under illumination. The *J-V* characteristics are in practical cases modeled according to the ideal diode equation (1), which for accounts for the shunt and series resistances [20],

$$J = J_L - J_s \exp\left[\frac{V+R_sJ}{mV_T}\right] - \sigma V \quad (1)$$

where J, J_L, J_s, V, m, V_T, R_s, J, and σ are the ideal current density, the current density from the source (in this work, it is the photo-generated current density, J_{ph} and will be referred to as such), the saturation current density, voltage across the PV terminals, the ideality factor, series resistance and shunt conductance respectively.

In the dark, an applied voltage, known also as the bias voltage generates current density in the opposite direction to the one generated by light. This current density is known as the dark current density and is computed from the equation [21] [20],

$$J_{dark} = -J_s\, exp\left[\frac{V+R_sJ}{mV_T}\right] - \sigma V \quad (2)$$

where J, J_{dark}, J_s, V, m, V_T, R_s, J, and σ are the ideal current density, the dark current density, the saturation current density, voltage across the PV terminals of the PV device, the ideality factor (=1 for an ideal PV device or ≠1 for a non-ideal PV device), series resistance and shunt conductance respectively.

Under illumination, the *J-V* characteristics are described by the equation [22] [20],

$$J = J_{ph} - J_s \exp\left[\frac{V+R_sJ}{mV_T}\right] - \sigma V \quad (3)$$

where J, J_{ph}, J_s, V, m, V_T, R_s and σ are the ideal current density, the photo-generated current density, thesaturation current density, voltage across the PV device terminals, the ideality factor (=1 for an ideal device or ≠1 for a non-ideal device), the thermal voltage, series resistance and shunt conductance respectively.

Setting of the ideality factor in equation (1) to one is the ideal case that assumes that all recombinations in the PV device occur via the band to band or the bulk areas of the PV device – not in the junction. The ideality factor describes how closely the PV device follows the ideal case scenario. In practical cases, PV devices are non-ideal since recombinations occur in other ways and areas of the devices other than only via band to band or in the bulk area of the devices. These devices yield ideality factors that deviate from the ideal.

From equations (2) and (3), the dark current density and photo-generated current density (respectively) can be plotted as functions of the applied bias voltage. This results in a curve typically known as the current density-voltage (*J-V*) characteristic curve. From the *J-V* curve, key parameters; V_{oc}, J_{sc}, J_s, FF, R_s, R_{sh} can be extracted and, m and η computed.

V_{oc} is the voltage measured when the terminals of a PV device are isolated. It relates to the condition when the potential difference is at its maximum value. At this point, dark current density and short circuit photo-current densities exactly cancel out and no flow of current is observed between the PV terminals. Setting J to zero in equation (3) and rearranging yields equation (4) that can be used to compute the photo-generated current, J_{ph}.

$$J_{ph} = J_s \exp\left[\frac{V}{mV_T}\right] \quad (4)$$

where J_{ph}, J_s, V m, and V_T are the photo-generated current density, the saturation current density, voltage across the PV device's terminals, the ideality factor and the thermal voltage respectively.

When V is maximum, i.e., V=V_{oc}, equation (4) leads to,

$$J_{ph} = J_s \exp\left[\frac{V_{oc}}{mV_T}\right] \quad (5)$$

where J_{ph}, J_s, V_{oc}, m, V_T and σ are the photo-generated current density, the saturation current density, the open circuit voltage, the ideality factor, thermal voltage and shunt conductance respectively.

Making V_{oc} the subject in equation (5) yields (6), which describes the voltage at zero current. This is the open circuit voltage,

$$V_{oc} = mV_T ln\frac{J_{ph}}{J_s} \quad (6)$$

where J_{ph}, J_s, V_{oc}, m and V_T are the photo-generated current density, the saturation current density, the open circuit voltage and the ideality factor and the thermal voltage respectively.

J_{sc} describes the photo-generated charge carriers, which in the case of exposure of the PV device to light is the light-generated current density. It is measured at the condition when the applied voltage is zero. Essentially, this is the current measured when the circuit is shorted and both the load and power are zero. If we set the applied voltage, V to zero and J to J_{sc} in equation (3), we obtain,

$$J_{sc} = J_{ph} - J_s \quad (7)$$

where J_{sc}, J_{ph}, and J_s are the short circuit current density, the photo-generated current density and the saturation current respectively.
This implies that,

$$J_{sc} \equiv J_{ph} \quad (8)$$

where J_{sc} and J_{ph} are the short circuit current density and the photo-generated current density respectively.

The actual current that flows out of a solar PV device is the ideal current, i.e., the short-circuit current density, minus the current that flows through the diode or dark current density, J_{dark},

$$J = J_{sc} - J_{dark} \quad (9)$$

where J, J_{sc} and J_{dark} are the ideal current density, the short circuit current density and the dark current density respectively.

FF is generally influenced by the series and shunt resistances. It is a measure of the squareness of the *J-V* curve and hence the quality of the solar PV device. It is defined as the ratio. It is determined from equation [22],

$$FF = \frac{P_m}{V_{oc}J_{sc}} = \frac{J_{mp}V_{mp}}{V_{oc}J_{sc}} \quad (10)$$

where *FF*, P_m, V_{oc}, J_{sc}, J_{mp} and V_{mp} are the fill factor, maximum power, the open circuit voltage, the short circuit current density, the maximum power current density and the maximum power voltage respectively.
A PV device's maximum power (P_m), maximum power current density (J_{mp}) and maximum power voltage (V_{mp}) are be extracted from a *P-V* curve. There exists a certain potential between the J_{sc} and V_{oc} on the *J-V* curve where P_m is found. At this point, the solar PV device delivers the highest power output (P_m). Voltage at this point is known as the maximum power voltage, while the current density is known as the maximum power current density. P_m, V_{mp}, J_{mp} can also be computed as shown in equations (11), (12) and (13),

$$P_m = FFV_{oc}J_{sc} \quad (11)$$

$$V_{mp} = \frac{FFV_{oc}J_{sc}}{J_{mp}} \quad (12)$$

$$J_{mp} = \frac{FFV_{oc}J_{sc}}{V_{mp}} \quad (13)$$

where P_m, *FF*, V_{oc} , J_{sc}, J_{mp} and V_{mp} are the maximum power, the fill factor, the open circuit voltage, the short circuit current density, the current density at maximum power and the voltage at maximum power respectively.

η is associated with the overall performance of the PV device. It is defined as the ratio of P_m to the power of incident radiation (P_{in}), which is given by the equation [20],

$$\eta = \frac{P_m}{P_{in}} = \frac{J_{mp}V_{mp}}{P_{in}} = \frac{V_{oc}J_{sc}FF}{P_{in}}x100\% \quad (14)$$

where η, P_m, J_{mp} , V_{mp} , V_{oc}, J_{sc} *FF*, and P_{in} are the efficiency, the maximum power, the maximum power current density, the maximum power voltage, the open circuit voltage, the short circuit current density, the fill factor and the power of the light that is incident on the PV device respectively.

B. Experimental

1) Materials

One functional dye-sensitized solar module was used in this study. The module; Omny 11200 outdoor module - model number HS Code 85414090 was used as supplied by G24 Innovations Limited (UK). It was made up of 11 cells, rated 0.5 Watts peak and 8 Volts. The cells were 1.5 inches thick and of a 15.92 cm^2 active area each; bringing the total active area of the module to 175.12 cm^2. The other apparatus used in the study were a tilt-able metal rack supplied by Solargent Limited, Kenya, 6 cm immersion thermometer supplied by Griffin & George Limited, UK, a GTH 1160 NiCr-Ni digital thermocouple supplied by TC limited, UK, a Raytek® *Plus* laser beam thermometer supplied by Raytek, USA, a CM3 pyranometer supplied by Kipp & Zonen, Delft/Holland, a Haenni solar 130 radiation meter supplied by Jenensfort, Switzerland, a DT9205A$^+$ digital multimeter supplied by Taurus Electronics Limited, Kenya, a Tektronix TDS 3032 digital phosphor oscilloscope supplied by

Tektronix inc., USA, a Keithley 2400 digital source meter supplied by Keithley inc., USA and a Laboratory Virtual Engineering Workbench (LabVIEW™) application software supplied by National Instruments inc., USA, a desktop computer supplied by Hewlett-Packard (HP), Kenya and an IEEE-488 GPIB cable supplied by National Instruments inc., USA.

2) J-V characterization under illumination

The module sample was fixed on the tilt-able metal rack and the CM3-pyranometer positioned in the plane of array with the module as shown in figure 4.3. The set-up was positioned on the roof-top of the Department of Physics, University of Nairobi at a suitable place where shadows could not be cast on either the module or the pyranometer. The module was connected to the Keithley 2400 Source Meter using alligator clips The Keithley source meter was connected to the HP desktop computer via an IEEE-488 GPIB interface. The computer was installed with LabVIEW™ application software. To the pyranometer, the DT9205A+ digital multimeter was connected to facilitate acquisition of irradiance data. Figure 2 illustrates how the experiment was set up.

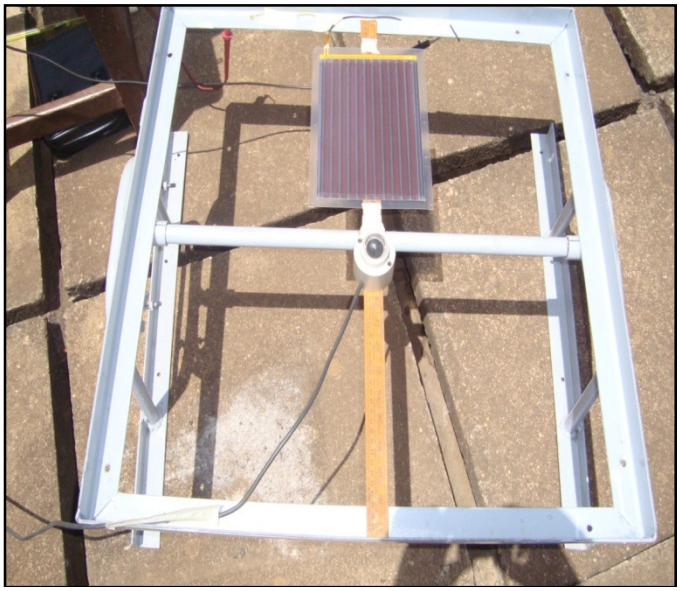

Figure 1: Picture of the module and pyranometer set-up

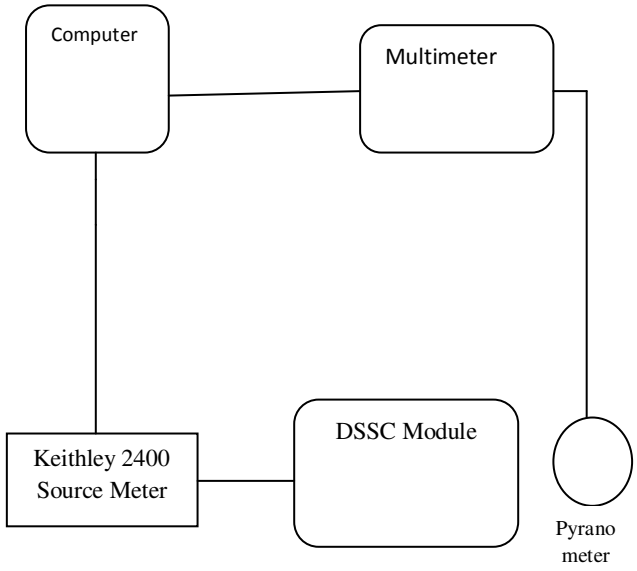

Fig .2 I-V characterization experimental set-up

Current-voltage readings were first acquired at normal incidence to the incoming solar beam radiation by varying the tilt to coincide with the optimum tilt angle at the period. Optimum tilt angle was obtained from the air mass *versus* optimum tilt angle curve.

Both the ambient and module temperatures at the time of the *I-V* measurement acquisition were recorded. Ambient temperatures were measured using the 6 cm immersion thermometer – measurements that were corroborated with those from the Kenya Meteorological department and NASA.

Module temperatures were obtained by attaching the GTH 1160 NiCr-Ni digital thermocouple sensor to the back side of the module recording the reading. Readings from the thermocouple sensor were checked by simultaneously point a laser beam from the Raytek® *Plus* laser beam thermometer at about one meter perpendicular to the module and obtaining the temperature reading on top of the module.

III. RESULTS AND DISCUSSION

Current density, *J* was observed to increase with radiation intensity. This behavior can be linked to the increasing number of photons that led to an increase in the number of excited electrons with more energy than the work function of the dye upon sensitization. These photo-excited electrons then escape into the semiconductor's conduction band and are collected at the load as current.

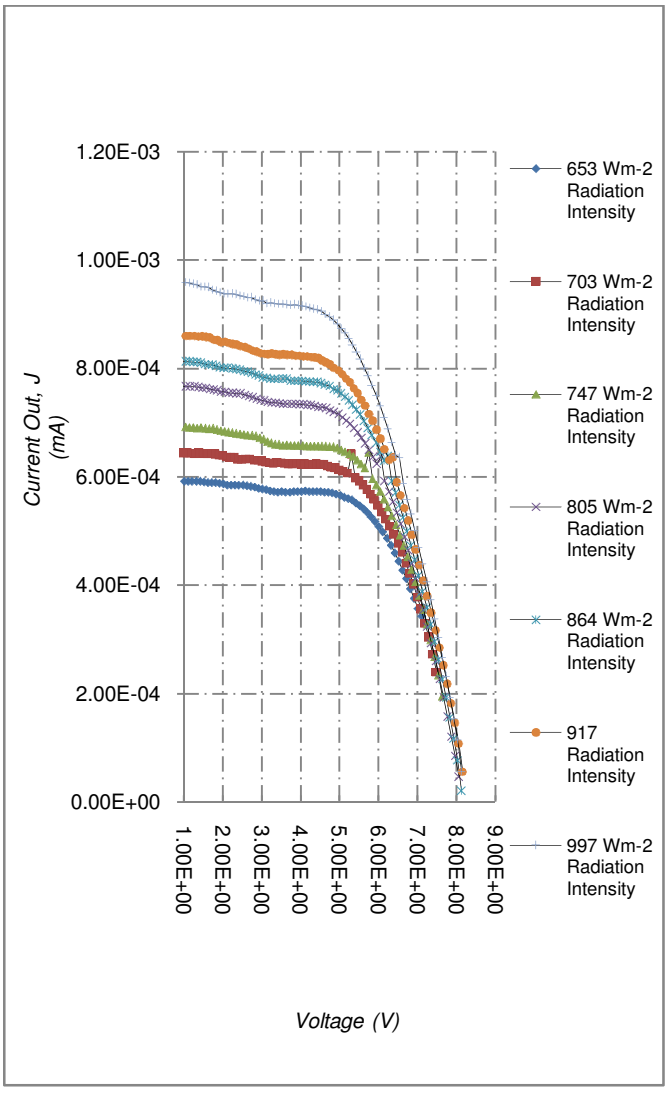

Fig .3 *I-V* characteristics for the module at different radiation intensities

Figure 6 shows how *FF*, V_{oc}, J_{sc} and η were affected by the variations in the irradiance intensity. it is observed that the module's short circuit current density, J_{sc} and the irradiance intensity are correlated. This is in agreement with with equation 9 and shows that the actual current flowing out of the solar PV device is the ideal current. However, J_{sc} values were very low for the module, which may imply that the electron recombinations through the electrolyte and during collection at the transparent conducting oxide (TCO) are high in the module. Reduction in *FF* has been observed at high irradiance levels. This shows the large series resistance (R_s) of the module.

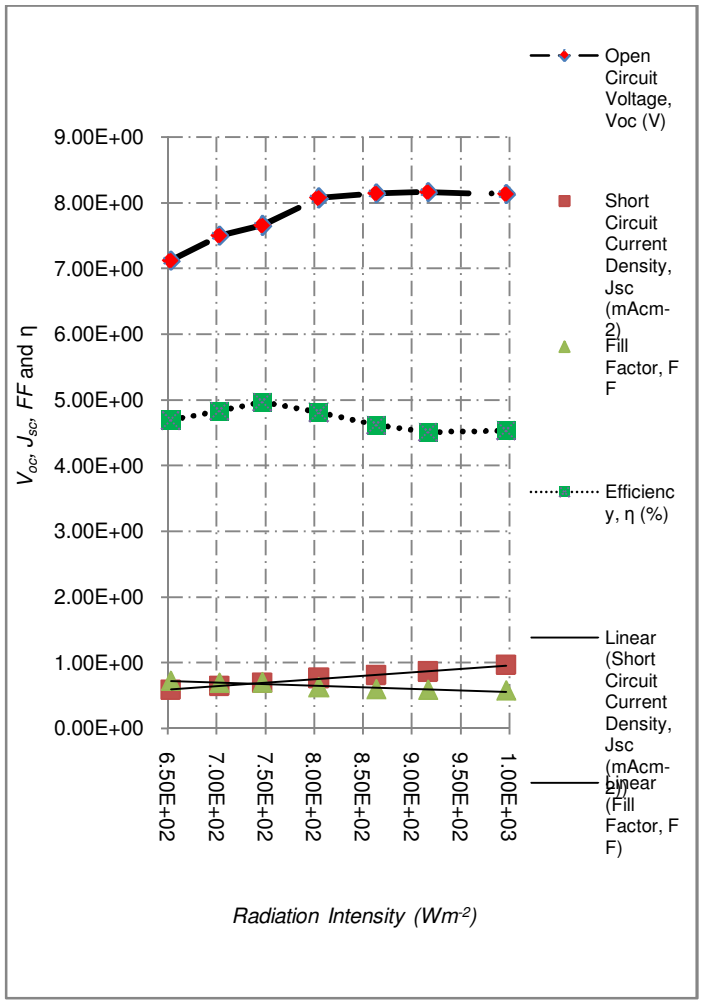

Fig .4 Relationship of V_{oc}, J_{sc}, *FF* and η as functions of irradiance intensity

Better relative efficiencies are observed at lower irradiance intensities as compared to the higher irradiance intensities. V_{oc} increased exponentially with irradiance intensity up to about 850 Wm^{-2} after which it remained constant upon further increase in irradiance intensity. This may be linked to the thin film nature of the module's cells, where the electron density in the conduction band of the semiconductor is high due to the high injection levels owing to the closeness of the injection to the collection - leading to a quick build-up of charges that exponentially raise V_{oc}. The constant V_{oc} after 850 Wm^{-2} may be linked to a state of equilibrium that arises after some period of time between photo-generation and recombination processes.

Figure 7 shows how the module performed at various module temperatures. As temperature increased, Rs→0. This shows that the module had an overall benefit from elevated temperatures as P_{max} is higher at higher module temperatures.

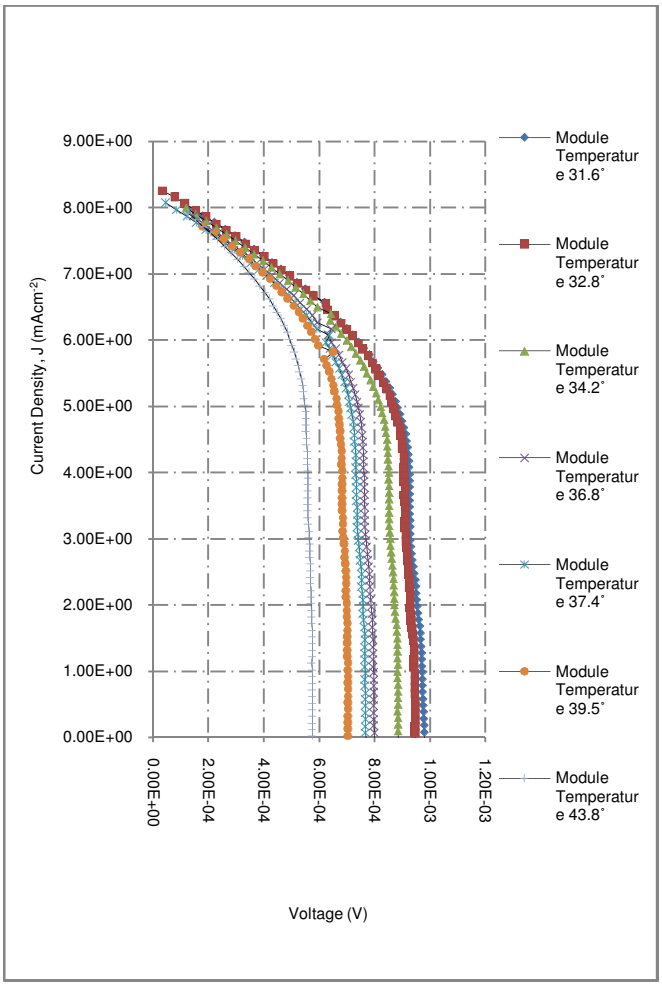

Fig .5 *I-V* characteristics of the DSSC module at different module temperatures.

Figure 8 shows how the fill factor, *FF*, *Voc* and η varied with temperature changes. There is a monotonic decrease in V_{oc} with increase in cell temperature that leads to a monotonic decrease in the solar-to-electricity conversion efficiency, η. The relative temperature dependence of V_{oc} and *FF* is however smaller. It can therefore be stated that the temperature dependence of η is dominated by the factors that affect J_{sc}. The trend of the results on η and module temperature may be linked to the limiting process of the tri-iodide diffusion, which limits J_{sc}.

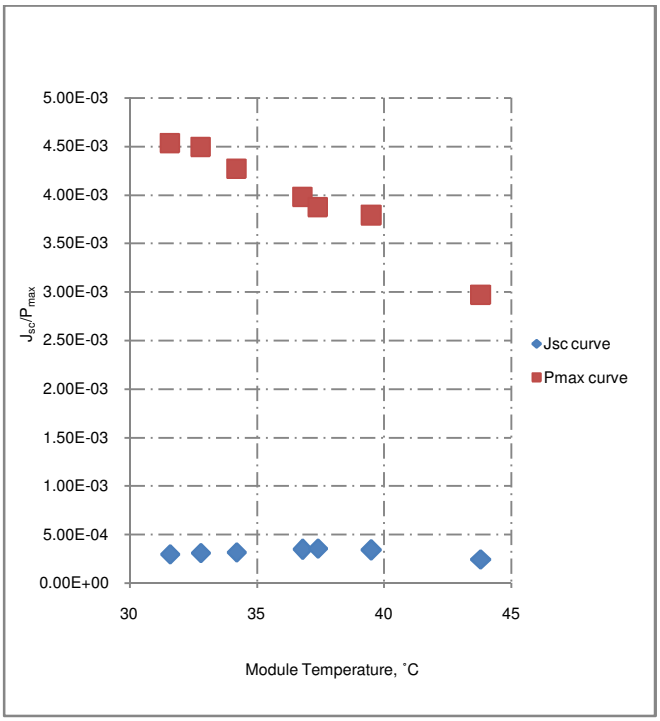

Fig .6 Relationship of J_{sc} and P_{max} as functions of module temperature.

J_{sc} increases with increasing temperature up to some point before starting to decrease. This J_{sc} increase behavior of the module at low module temperatures can be attributed to the diffusion of the tri-iodide which limits J_{sc}, while at increased cell temperatures, according to Arrhenius law according to which the diffusion coefficient exponentially increases with increasing temperature there is an observed increase in short circuit current density, J_{sc}. Nonetheless, the decrease that is observed after about 40˚C module temperature can be attributed to the possibility of recombinations at higher temperatures leading to reduction in current collection.

These limiting processes are linked to type and concentration of electrolyte components as is evident from the experiment by [23], which showed that when I_2 and consequently the tri-iodide concentration is low in the measured temperature window of 5-50˚C firstly, J_{sc} increases with temperature, reaches a maximum but later, further increase in temperature leads to decrease in J_{sc} [23].

IV. CONCLUSION

Effects of temperature and irradiance intensity on a dye-sensitized solar module's performance have been investigated in a temperate tropical area, 1.28˚ South and 35.82˚ East, Nairobi, Kenya. The results show better relative efficiencies for the module at lower irradiance intensities as compared to higher irradiance intensities. V_{oc} increased with increase in irradiance intensity up to 850 Wm^{-2} after which it remained constant with further irradiance intensity increase.

The increase in V_{oc} with increase in irradiance intensities can be attributed to the high injection levels that emanates from the closeness of the injection to the collection - leading to a quick build-up of charged that exponentially raise the open circuit voltage. This is due to the thin film nature of the module's cells. On the other hand, the constant V_{oc} observed from irradiance intensities > 850 Wm^{-2} may be linked a state of equilibrium that arises after some period of time between photo-generation and recombination processes.

J_{sc} of the module sample was found to be very small. It however correlated with irradiance intensity. The small J_{sc} values can be attributed to high levels of electron recombination through the electrolyte and during collection at the transparent conducting oxide in the module. Reduction in the fill factor was also observed at high irradiance intensities, indicating the large series resistance of the module.

An overall benefit from elevated module temperatures was observed as the maximum power increased with increasing module temperatures and irradiance intensity. V_{oc} for the module showed a monotonic decrease with increase in temperature leading to a monotonic decrease in efficiency. The temperature dependence of V_{oc} and fill factor were however very small, which implies that the temperature-dependence of efficiency for the module was dominated by factors that affect the J_{sc}. These include the diffusion of the tri-iodide that limits J_{sc} at low temperatures but leads to increases in J_{sc} at higher temperatures in accordance with Arrhenius law. The decrease in J_{sc} after about 40˚C module temperature can be attributed to the possibility of recombinations at higher temperatures.

The relatively better efficiencies observed for the dye-sensitized solar module at low irradiance intensities together with its ability to benefit from elevated temperatures under high illumination place dye-sensitized solar modules in a remarkable position for use in the temperate tropics. The design of energy efficient building facades for the temperate tropics stands to benefit immensely from these findings.

REFERENCES

[1] Leng, R., (2005). Implications of the decline in world oil reserves for future world livestock production. *School of Rural Science and Agriculture, University of New England,* p. 95 – 105.

[2] Aleklett, K., (2007). Reserve driven forecasts for oil, gas and coal and limits in carbon dioxide emissions. *In discussion paper number 2007-18. Joint Transport Research Centre,* p. 1 – 20.

[3] Hahn, R., Litan, R. and Singer, H., (2007). The economics of 'wireless net neutrality'. *American Enterprise Institute (AEI) – Brookings Joint Centre for Regulatory Studies,* p. 1 – 54.

[4] Barnes, D. and Toman, M., (2006). Energy, equity and economic development. *In economic development and environmental sustainability. Oxford University Press,* p. 1 – 52.

[5] Heymann, E. (2011). Carbon capture and storage for climate protection – important, tedious and costly. *Deutsche Bank,* p. 1 – 5.

[6] Dincar, I., (2003). The role of energy in energy policy making. *Energy Policy,* 30, p. 137 – 149.

[7] IPCC. 2007., (2007) "Climate change 2007: The physical science basis: Summary of policy makers". *Intergovernmental Panel on Climate Change Secretariat*.

[8] IEA, (2007). Key world energy statistics 2007. *International Energy Agency, 2007.*

[9] Muoghalu, J. (2003). Priority parameters: Abiotic and biotic components. *In environmental monitoring (edited by Inyang, H. and Daniels, J.). Encyclopaedia of Life Support Systems (EOLSS),* p. 1 – 8.

[10] Richards, B. and Schäfer, A. (2009). Renewable energy to power water treatment systems. *Elsevier*, p. 353 – 374.

[11] Kuhlbrodt, T., Griesel, A., Montoya, M., Levermann, A., Hofmann, M. and Rahmstorf, S., (2006). On the driving processes of atlantic meridional overtuning circulation. *Potsdam Institute for Climate Research,* p. 1 – 69.

[12] Quaschning, V., (2005). "Understanding Renewable Energy Systems". *Earthscan Canada*. 1-3.

[13] Lewis, N. and Crabtree, G., (2007). Solar energy conversion. *Physics Today*, 60, p. 37 - 42.

[14] Bakas, I., (2011). Solar energy/photovoltaics. *In solar energy and housing – Corpus. Copenhagen Resource Institute (CRI)*, p. 1 – 6.

[15] Krugmann, P., (2011). That's right: Solar power is now cost-effective. *The Seattle Times,* [retrieved on 23rd March, 2012 at http://seattletimes.nwsource.com/html/opinion].

[16] Gunerhan, H., Hepbasli, A. and Giresunlu, U., (2009). Environmental impacts from solar energy systems. *Energy Sources,* A, 31, p. 131 – 138.

[17] Whitney, Jr., (2010). Significant sustainable energy systems. *In clean energy action project. Solar PV Energy,* p. 1 – 36.

[18] Saga, T., (2010). Advances in crystalline silicon solar cell technology for industrial mass production. *NPG Asia Materials,* 2, p. 96 – 102.

[19] O'Regan, B. and Grätzel, M., (1991). A low cost, high efficiency solar cell based on dye sensitised colloidal TiO_2 films. *Nature*, 353, p. 737 - 739.

[20] Hedegus, S. and Shafarman, N., (2004). Thin film solar cells: Device Measurement and Analysis. *Progress in Photovoltaic Research and Application*, 12, 155-176.

[21] Sze, S. M., (1981). "Physics of semiconductor devices". *New York: Wiley International Publishers Inc.*122 - 124.

[22] Simiyu, J., (2010). "Characterization of Anthocyanin Dyes and Investigation of Charge Transport in TiO_2 Dye Sensitized Solar Cells". *Ph.D thesis for the University of Nairobi*. 1 - 13.

[24] Berginc, M., Krašovec, U. O., Hočevar, M. and Topič, M., (2008). Performance of dye-sensitized solar cells based on ionic liquids:

Effect of temperature and iodine concentration. *Thin Solid Films,* 516, p. 7155 – 7159.

Raphael Venson Makokha Otakwa is a postgraduate student (Physics) at the University of Nairobi, Kenya. He is a registered solar energy applications practitioner in Kenya and holds a Master of Science (M.Sc.) in Physics (condensed matter and solar energy) from the University of Nairobi. His research interests are in solar energy materials and applications.